Stoch Environ Res Risk Assess (2006) 21: 131–141
DOI 10.1007/s00477-006-0050-9

ORIGINAL PAPER

Chulsang Yoo · Sangdan Kim · Tae-Woong Kim

Assessment of drought vulnerability based on the soil moisture PDF

Published online: 26 April 2006

Abstract This paper studies the statistics of the soil moisture condition and its monthly variation for the purpose of evaluating drought vulnerability. A zero-dimensional soil moisture dynamics model with the rainfall forcing by the rectangular pulses Poisson process model are used to simulate the soil moisture time series for three sites in Korea: Seoul, Daegu, and Jeonju. These sites are located in the central, south-eastern, and south-western parts of the Korean Peninsular, respectively. The model parameters are estimated on a monthly basis using hourly rainfall data and monthly potential evaporation rates obtained by the Penmann method. The resulting soil moisture simulations are summarized on a monthly basis. In brief, the conclusions of our study are as follows. (1) Strong seasonality is observed in the simulations of soil moisture. The soil moisture mean is less than 0.5 during the dry spring season (March, April, and June), but other months exceed the 0.5 value. (2) The spring season is characterized by a low mean value, a high standard deviation and a positive skewness of the soil moisture content. On the other hand, the wet season is characterized by a high mean value, low standard deviation, and negative skewness of the soil moisture content. Thus, in the spring season, much drier soil moisture conditions are apparent due to the higher variability and positive skewness of the soil moisture probability density function (PDF), which also indicates more vulnerability to severe drought occurrence. (3) Seoul, Daegue, and Jeonju show very similar overall trends of soil moisture variation; however, Daegue shows the least soil moisture contents all through the year, which implies that the south-eastern part of the Korean Peninsula is most vulnerable to drought. On the other hand, the central part and the south-western part of the Korean peninsula are found to be less vulnerable to the risk of drought. The conclusions of the study are in agreement with the climatology of the Korean Peninsula.

Keywords Drought · Soil moisture · Seasonality · PDF

C. Yoo (✉)
Department of Civil and Environmental Engineering,
Korea University, 5-1 Anam-dong, Sungbuk-gu,
Seoul 136-701, South Korea
E-mail: envchul@korea.ac.kr
Tel.: +82-2-32903321
Fax: +82-2-9287656

S. Kim
Department of Environmental System Engineering,
Pukyong National University, 599-1 Daeyon-dong,
Nam-gu, Busan 608-737, South Korea
E-mail: skim@pknu.ac.kr

T.-W. Kim
Department of Civil and Environmental System Engineering,
Hanyang University, 1271 Sa-1 dong, Sangnok-gu, Ansan,
Kyeonggi-do 426-791, Korea
E-mail: twkim72@hanyang.ac.kr

1 Introduction

Korea, located in the Asian Monsoon Region, shows a typical seasonal pattern in its climate. Four seasons are developed due to the change of its temperature and rainfall amount. The dry season includes most of spring, fall, and winter, and the wet season of summer. June, July, August, and September are generally included in the wet season in Korea.

More than 60% of the total annual precipitation is concentrated in the wet summer season, so flooding has become an annual event in the Korean Peninsula (Han and Byun 1994; KOWACO 2002). Monsoon lasts about a month from mid-June to July, and several typhoons hit the Korean peninsula from late August to September. Convective storms are also frequently developed locally to cause flash floods. Hot and humid weather lasts about 2 months during this wet summer season.

On the other hand, a long dry spell continues until the monsoon season begins. Almost every 2 years, the Korean Peninsula suffers from a shortage of rain, nee-

ded mostly for agricultural use, which sometimes turns into a very deadly one lasting more than 2 years. Many attempts have been tried to quantify the drought, to assess the damage of drought, and to develop measures to overcome the drought, most of which have been based on precipitation data analysis (Byun 1996; Rhee 1998; KOWACO 2002). Almost nothing in evaluation and characterization has been done about the soil moisture condition. No structured survey or measurement of the soil moisture has been conducted locally or nationwide.

Soil moisture covers a small part of the hydrologic cycle linking rainfall, runoff, and groundwater fluctuations, and thus it has received little attention from hydrologists until recently. However, soil moisture plays an important role for connecting land surface processes to the atmospheric processes. Soil moisture is continuously recharged by the intermittent rainfall and depleted by runoff, deep infiltration, and evapotranspiration (Bell et al. 1980; Entekhabi and Rodriguez-Iturbe 1994; Castelli and Rodriguez-Iturbe 1996; Entekhabi et al. 1996; Yoo et al. 1998, 2001). Agricultural productivity is also highly dependent on the water supply from soil as a form of soil moisture. Thus, soil moisture should be understood to gain a better insight on the drought and its characteristics.

The characteristics of soil moisture can be summarized statistically, ultimately as a form of the probability density function (PDF). Basically, the characterization of a soil moisture field requires a large amount of intensive measurements. However, due to the lack of data, this characterization becomes impossible in most cases. Alternatively, one may rely on a modeling study to derive the characteristics of soil moisture, which, in turn, will be used for planning (or, designing) a larger scale observation (Jackson and Le Vine 1996; Njoku and Entekhabi 1996). Examples of related studies can be found in Yoo et al. (1998, 2001, 2005). They attempted to characterize the temporal behavior of the soil moisture field both in space (Yoo et al. 1998, 2001) and in time (Yoo et al. 2005). Yoo (2001) also showed several sampling schemes and related errors for the soil moisture sampling.

In this study, authors try to statistically quantify and evaluate the condition of soil moisture as well as its seasonality. The ultimate goal of this study is to derive the PDF of the soil moisture to gain a better insight for the analysis of drought. A zero-dimensional soil moisture dynamics model (Entekhabi and Rodriguez-Iturbe 1994) with the rainfall forcing by the rectangular pulses Poisson process model (Rodriguez-Iturbe et al. 1984) is used for this study. First- and second-order moments of soil moisture are also reviewed for both instantaneous and locally averaged cases to link these moments to those of the rainfall, a linking which can be used to evaluate the impact of rainfall on the soil moisture. Finally, a simulation study is carried out to estimate the PDF of soil moisture as well as to evaluate its seasonality.

2 Review of soil moisture and rainfall model

2.1 A model for soil moisture dynamics

Entekhabi and Rodriguez-Iturbe (1994) proposed a model for soil moisture dynamics by adopting the linear reservoir concept and considering the diffusion effect on the soil moisture propagation. The model assumes that the soil moisture s (dimensionless) obeys a linear stochastic partial differential equation like

$$nZ_r \frac{\partial s}{\partial t} = -\eta s + nZ_r\left(\kappa \nabla^2 s\right) + P \tag{1}$$

where, n is the soil porosity (dimensionless); Z_r is the depth of the soil top layer (L); κ is the diffusion coefficient (L^2/T); η is defined as the loss coefficient with dimension of (L/T); and P is the rainfall intensity (L/T). The initial high variability in s, originated from P both in time and space, becomes smoothed in space by the diffusion process.

This equation represents the dynamics of the soil moisture field. Entekhabi and Rodriguez-Iturbe (1994) also analyzed the model based on the Fourier analysis and derived the relationship between the soil moisture spectrum and the noise-forcing spectrum (i.e., the rainfall spectrum)

$$\Phi_{ss}(v,\omega) = G(v,\omega)\Phi_{pp}(v,\omega) \tag{2}$$

where, Φ_{ss} is the soil moisture spectrum; Φ_{pp} is the rainfall spectrum; $G(v,\omega)$ is the gain function of wave number v and frequency ω, which is

$$G(v,\omega) = \frac{(1/nZ_r)^2}{\left[4\pi^2\kappa v^2 + (\eta/nZ_r)\right]^2 + 4\pi^2\omega^2}. \tag{3}$$

In our study the emphasis is on the analysis of temporal behavior of soil moisture, so the diffusion effect in space is not considered and the model becomes

$$nZ_r \frac{\partial s}{\partial t} = -\eta s + P \tag{4}$$

The gain function also becomes simplified such as:

$$G(\omega) = \frac{1}{\eta^2 + 4\pi^2 n^2 Z_r^2 \omega^2} \tag{5}$$

2.2 Rainfall forcing

The model used for representing rainfall intensity P is the rectangular pulses Poisson process model proposed by Rodriguez-Iturbe et al. (1984). This model was developed with the following assumptions. Rainfall events occur according to a Poisson process with parameter λ, and each event is characterized by a rectangular pulse of height i_r and duration t_r. It is also assumed that the event characteristics are independent of the time of occurrence and, furthermore, that they are

identically distributed and mutually independent random variables. In a simplest case, i_r and t_r for each event are also assumed to be independent. This last assumption has been commonly made in the application of this model for representing P to make the analytical derivation of second-order moment tractable, although it may be unrealistic (Cordova and Rodriguez-Iturbe 1985). In this study we also assume that in each event, i_r and t_r are independent and that i_r and t_r follow exponential density functions given by

$$f(i_r) = \mu e^{-\mu i_r} \quad \mu>0 \tag{6}$$

$$f(t_r) = \theta e^{-\theta t_r} \quad \theta>0 \tag{7}$$

The second-order characterization of the rainfall intensity process P is given by Rodriguez-Iturbe et al. (1984):

$$E[P(t)] = \frac{\lambda}{\mu\theta} \tag{8}$$

$$\mathrm{Var}[P(t)] = \frac{2\lambda}{\theta\mu^2} \tag{9}$$

$$\mathrm{Corr}[P(t), P(t+r)] = \rho(\tau) = e^{-\theta\tau}, \quad \tau>0. \tag{10}$$

Note that the Markovian structure of the correlation function which depends only on the mean duration θ^{-1} of rainfall events, and other parameters λ and μ do not play any role.

Rodriguez-Iturbe et al. (1984) also give the moments of the aggregated process P_T over the aggregation period T. The mean and variance are

$$E[P_T(t)] = \frac{\lambda}{\mu\theta} \tag{11}$$

$$\mathrm{Var}[P_T(t)] = \frac{4\lambda}{\theta^3\mu^2T^2}\left(\theta T - 1 + e^{-\theta T}\right) \tag{12}$$

$$\mathrm{Cov}[P_T(1), P_T(n)] = \frac{2\lambda}{\theta^3\mu^2T^2}\left(1 - e^{-\theta T}\right)^2 e^{-(n-2)\theta T}, \quad n \geq 2. \tag{13}$$

This model has very restrictive properties regarding its use in hydrologic simulation, which are studied in detail by Rodriguez-Iturbe et al. (1984). Especially, what the authors want to mention here is that in order to preserve the historical characteristics of the rainfall data at a certain level of aggregation, (e.g., 1 h), it is necessary to estimate the parameters λ, μ, and θ from the equations of the same aggregated process P_T. These parameters will be greatly different from those estimated at another levels of aggregation (e.g., 6 h, 1 day, etc.) [see Rodriguez-Iturbe (1986) for more detailed information].

2.3 Statistics of combined rainfall–soil moisture model

Derivation of second-order statistics of soil moisture is required for the extensive evaluation of the soil moisture evolution. Yoo et al. (2005) derived the covariance function and spectrum of the combined rainfall–soil moisture model to evaluate the effect of rainfall on soil moisture statistics analytically. First, the mean and covariance function of the instantaneous process are as follows:

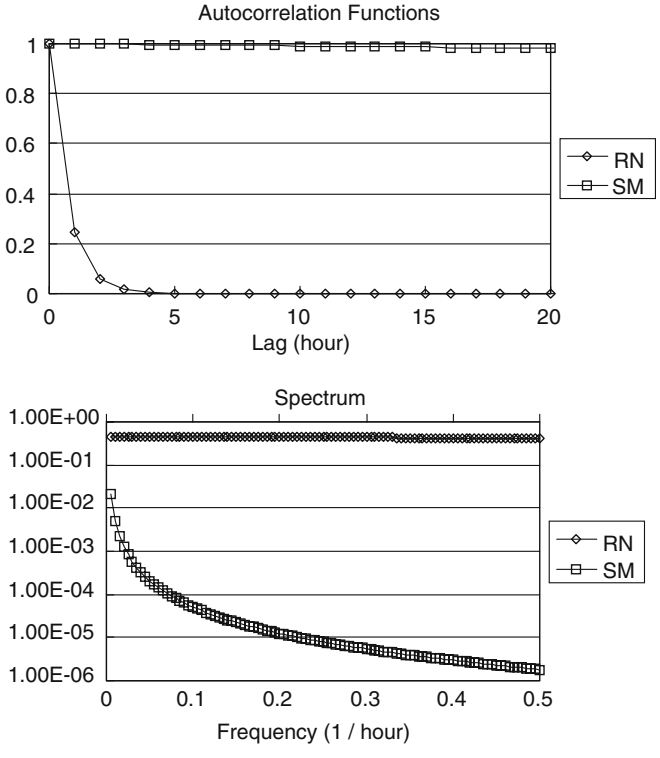

Fig. 1 Auto-correlation functions and spectrums of rainfall (*RN*) and soil moisture (*SM*) data (Monsoon 1990 Kendall South 1 data)

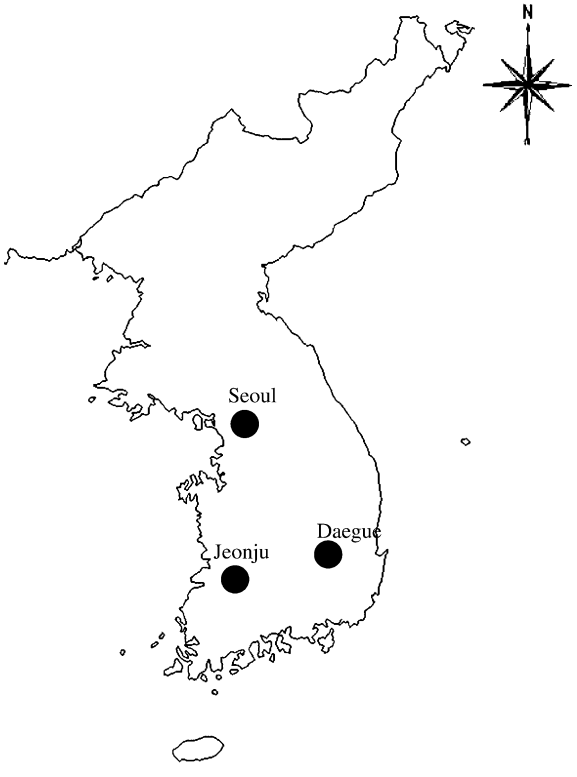

Fig. 2 Locations of Seoul, Daegue, and Jeonju in the Korean Peninsula

$$\mathrm{E}[S(t)] = \frac{\lambda}{\mu\theta \cdot nZ_r} \tag{14}$$

$$\mathrm{Var}[S(t)] = \frac{2\lambda}{\mu^2 \cdot n^2 Z_r^2}\left(\frac{\eta^2}{\theta^3\left(\eta^2/\theta^2 - n^2 Z_r^2\right)} + \frac{\eta}{\theta^2\left(nZ_r - \eta^2/nZ_r\theta^2\right)}\right) \tag{15}$$

$$\mathrm{Cov}[S(t), S(t+\tau)] = \frac{2\lambda}{\mu^2 \cdot n^2 Z_r^2}\left(\frac{\eta^2}{\theta^3\left(\eta^2/\theta^2 - n^2 Z_r^2\right)}\mathrm{e}^{-\theta\tau} + \frac{\eta}{\theta^2\left(nZ_r - \eta^2/nZ_r\theta^2\right)}\mathrm{e}^{-\eta\tau/nZ_r}\right). \tag{16}$$

For the locally (in time) averaged process, the mean is the same as in Eq. 14, but its variance and covariance become changed to consider the time-averaging effect.

$$\mathrm{Var}[S_T(t)] = \frac{4\lambda}{\mu^2 T^2 \cdot n^2 Z_r^2} \times \left(\frac{\eta^2}{\theta^5\left(\eta^2/\theta^2 - n^2 Z_r^2\right)}\left(\theta T - 1 + \mathrm{e}^{-\theta T}\right) + \frac{1}{\theta^2\left(\eta/nZ_r - \eta^3/n^3 Z_r^3\theta^2\right)} \times \left(\eta T/nZ_r - 1 + \mathrm{e}^{-\eta T/nZ_r}\right)\right) \tag{17}$$

$$\mathrm{Cov}[S_T(t), S_T(t+\tau)] = \frac{2\lambda}{\mu^2 T^2 \cdot n^2 Z_r^2} \times \left(\frac{\eta^2}{\theta^5\left(\eta^2/\theta^2 - n^2 Z_r^2\right)}\left(1 - \mathrm{e}^{-\theta T}\right)^2 \mathrm{e}^{-(\tau-1)\theta T}. + \frac{1}{\theta^2\left(\eta/nZ_r - \eta^3/n^3 Z_r^3\theta^2\right)}\left(1 - \mathrm{e}^{-\eta T/nZ_r}\right)^2 \times \mathrm{e}^{-\eta(\tau-1)T/nZ_r}\right), \quad \tau \geq 1. \tag{18}$$

Table 1 Basic statistics of rainfall as well as evaporation amount used for parameter estimation

Month	Mean, mm (1 h)[a]	Variance, mm^2 (1 h)	Lag-1 auto-correlation		Evaporation amount (mm)
			1 h	6 h	
Seoul					
Jan	0.026	0.06	−0.000	0.425	48.7
Feb	0.044	0.18	−0.000	0.534	63.8
Mar	0.077	0.56	−0.000	0.569	110.4
Apr	0.082	0.28	0.644	0.331	137.7
May	0.123	0.62	0.575	0.520	154.7
Jun	0.185	1.49	0.627	0.444	194.1
Jul	0.498	6.63	0.568	0.364	178.9
Aug	0.398	4.86	0.531	0.404	177.6
Sep	0.216	2.97	0.536	0.354	148.2
Oct	0.075	0.40	0.716	0.380	97.0
Nov	0.088	0.77	0.000	0.491	59.1
Dec	0.034	0.11	−0.000	0.377	44.6
Daegu					
Jan	0.042	0.16	−0.000	0.525	46.2
Feb	0.052	0.24	−0.000	0.439	65.8
Mar	0.084	0.50	0.002	0.452	113.8
Apr	0.088	0.34	0.764	0.463	142.5
May	0.098	0.60	0.310	0.235	164.6
Jun	0.179	1.12	0.634	0.456	214.2
Jul	0.301	2.70	0.497	0.375	188.5
Aug	0.260	2.69	0.522	0.418	184.8
Sep	0.159	1.08	0.620	0.433	152.4
Oct	0.036	0.14	0.513	0.426	101.7
Nov	0.037	0.18	−0.000	0.317	57.0
Dec	0.022	0.08	−0.000	0.587	41.2
Jeonju					
Jan	0.056	0.19	−0.000	0.515	45.9
Feb	0.068	0.29	−0.000	0.578	63.2
Mar	0.088	0.46	−0.000	0.462	112.7
Apr	0.090	0.32	0.751	0.460	138.1
May	0.100	0.36	0.560	0.336	159.9
Jun	0.210	1.76	0.594	0.409	215.7
Jul	0.364	4.31	0.451	0.308	186.9
Aug	0.326	4.12	0.441	0.288	183.4
Sep	0.188	1.89	0.475	0.357	150.2
Oct	0.062	0.26	0.496	0.400	99.6
Nov	0.068	0.29	−0.000	0.423	61.3
Dec	0.042	0.12	−0.000	0.326	42.5

[a]The level of aggregation

The spectral density function of the soil moisture is also useful for various applications. One good example application of this function is the evaluation of sampling errors due to intermittent sampling, either in space or in time as shown by North and Nakamoto (1989). The normalized spectrum $g(\omega)$, simply using the correlation function ρ (τ), can be derived using the relationship

$$g(\omega) = \frac{2}{\pi}\int_0^\infty \rho(\tau)\cos\omega\tau\,\mathrm{d}\tau. \tag{19}$$

Also, the following relation is useful for deriving the normalized spectrum for both instantaneous and locally averaged cases.

$$\int_0^\infty \mathrm{e}^{-ax}\cos bx\,\mathrm{d}x = \frac{\mathrm{a}}{\mathrm{a}^2 + b^2.} \tag{20}$$

Resulting equations of both spectrums are skipped here as they are simply the combinations of Eqs. 15 and 16, or Eqs. 17 and 18 along with Eq. 20, respectively.

2.4 Comparison of statistical structure of rainfall and soil moisture

The obvious difference between rainfall and soil moisture can be easily found in Fig. 1, which compares the auto-correlation functions and spectra of rainfall and soil moisture models with their parameters tuned to the Monsoon 1990 data (Kustas and Goodrich 1994).

In the comparison of auto-correlation functions, we can easily distinguish the two processes, one with a very highly correlated mechanism of soil moisture with its lag-1 (h) auto-correlation coefficient of almost 1.0 and the other with a much less correlated mechanism of rainfall with a slightly significant auto-correlation coefficient at lag-1 (h). Similar characteristics can also be found in the comparison of their spectrums. The rainfall spectrum shows a typical pattern of white noise or AR(1) model (auto regressive model of order 1) spectrum with a very small lag-1 (h) auto-correlation coefficient, a pattern which is the same interpretation given to the auto-correlation function. However, the soil moisture spectrum shows a low frequency dominant

Table 2 Rainfall and soil moisture model parameters estimated

Month	λ (1/h)	μ (mm/h)	θ (h)	η (mm/h)
Seoul				
Jan	0.0048	0.759	0.244	0.0655
Feb	0.0035	0.465	0.172	0.0949
Mar	0.0031	0.264	0.153	0.1484
Apr	0.0275	0.478	0.702	0.1913
May	0.0331	0.300	0.897	0.2079
Jun	0.0272	0.196	0.747	0.2696
Jul	0.0518	0.113	0.921	0.2405
Aug	0.0493	0.119	1.040	0.2387
Sep	0.0234	0.106	1.020	0.2058
Oct	0.0123	0.315	0.523	0.1304
Nov	0.0037	0.214	0.198	0.0821
Dec	0.0056	0.577	0.285	0.0599
Daegu				
Jan	0.00356	0.480	0.177	0.0621
Feb	0.00488	0.398	0.233	0.0979
Mar	0.00582	0.310	0.224	0.1530
Apr	0.0165	0.447	0.419	0.1979
May	0.0378	0.181	2.14	0.2212
Jun	0.0331	0.254	0.728	0.2975
Jul	0.0549	0.157	1.16	0.2618
Aug	0.0389	0.139	1.07	0.2484
Sep	0.0284	0.232	0.768	0.2048
Oct	0.0153	0.381	1.10	0.1367
Nov	0.00466	0.366	0.348	0.0792
Dec	0.00172	0.537	0.144	0.0554
Jeonju				
Jan	0.00561	0.546	0.183	0.0616
Feb	0.00451	0.449	0.148	0.0938
Mar	0.00681	0.357	0.217	0.1515
Apr	0.0195	0.484	0.446	0.1918
May	0.0393	0.416	0.946	0.2149
Jun	0.0326	0.184	0.841	0.2996
Jul	0.0555	0.113	1.35	0.2596
Aug	0.0473	0.105	1.39	0.2465
Sep	0.0322	0.137	1.25	0.2019
Oct	0.0239	0.331	1.17	0.1339
Nov	0.00715	0.430	0.245	0.0851
Dec	0.00859	0.605	0.337	0.0571

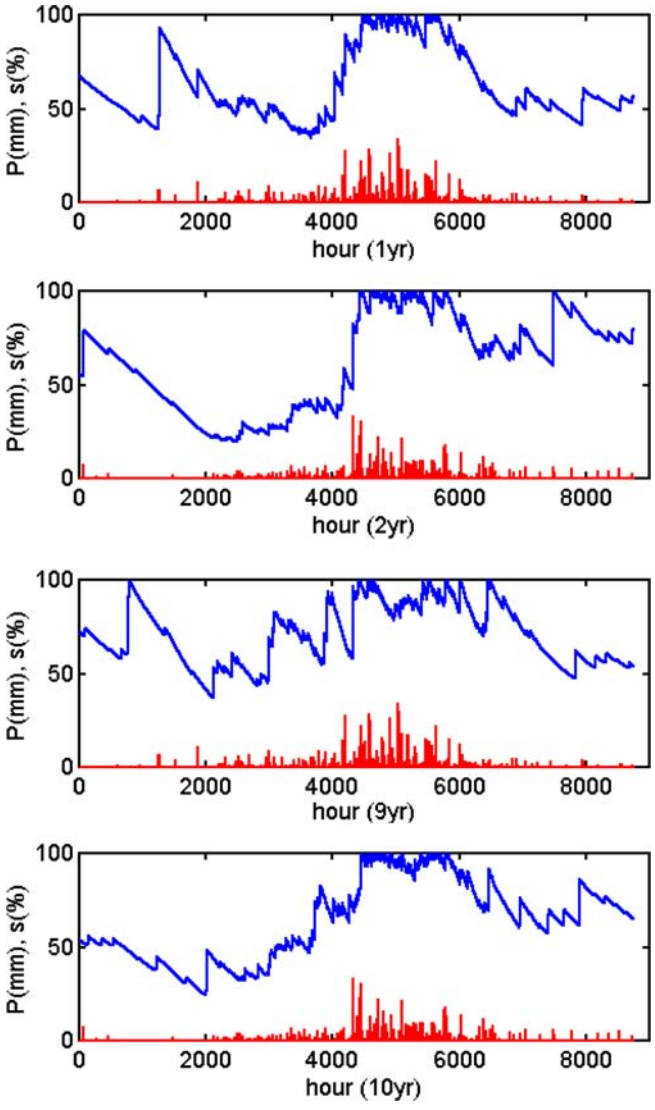

Fig. 3 Rainfall and soil moisture data generated for the Seoul site (*upper two panels* are for the first and second year, and the *lower two panels* for the 9th and 10th year)

shape like a long-memory process. This shape is due to the fact that the lag-1 (h) auto-correlation coefficient of soil moisture is almost 1.0. Also, we can see the obviously different (small) variance of soil moisture with that of rainfall.

3 Data and parameter estimation

Three sites in Korea (Seoul, Daegu, and Jeonju) were considered in this study. These sites are located in the central, south-eastern, and south-western part of the Korean Peninsular. Thus, by investigating these three sites we may get some idea about the drought in whole Korean Peninsula. These sites are located in the map of Korea (Fig. 2).

All the parameters were estimated on a monthly basis (that is, we assume that the parameters estimated remain the same through the month). Hourly rainfall data and monthly potential evaporation amounts estimated by the Penmann method were used for parameter estimation. Basically, the parameters of the rainfall model and the soil moisture model were estimated separately. Mean, variance, and lag-1 auto-correlation coefficient for 1-h rainfall data were used for the estimation of rainfall model parameters (λ, μ, and θ) by fitting them to Eqs. 11, 12, and 13. However, for January, February, March, November, and December, the lag-1 autocorrelation coefficients of 6-h aggregation level data were considered for the parameter estimation instead of 1-h aggregation level data. It was because the lag-1 auto-correlation coefficients for 1-h rainfall data of those months had been estimated to be too small (nearly zero) to be used for parameter estimation.

The soil moisture model parameter (that is, loss rate η) was assumed to be the potential evaporation rate estimated by the Penman method. As the loss rate η considers various loss mechanisms like evaporation, transpiration, surface runoff, deep percolation etc., it should be estimated to satisfy the annual water balance (Entekhabi and Rodriguez-Iturbe 1994). However, the monthly water balance may not be made mainly due to slow flows like the groundwater flow and interflow, so, in some months, it can be positive (surplus) or negative (deficit). Instead, in this study, the monthly estimate of potential evaporation was introduced to estimate the loss rate. That is, the loss rate of a month was decided by dividing the monthly potential evaporation amount estimated by the number of days of the month. The monthly potential evaporation amount was assumed to well represent the total monthly loss amount. Also, authors checked that the sum of all the monthly potential evaporation amounts was similar to the average annual rainfall amount.

The effective soil depth nZ_r was assumed to be 0.15 m (150 mm) in this study. In fact, the decision of nZ_r is rather subjective. Entekhabi and Rodriguez-Iturbe (1994) assumed the depth of the top soil layer Z_r to be 50 cm and the porosity n to be 0.3 (so the nZ_r becomes 0.15 m). The values adopted in this study were also based on the similar assumption. It is also true that the effective soil depth nZ_r assumed in this study may derive a bit biased soil moisture field; however, it had already been shown that the sensitivity of soil moisture field evolution to this parameter is much smaller than that to the rainfall arrival rate, a rainfall model parameter (Yoo et al. 2005).

The data used for the parameter estimation are summarized in Table 1, and the parameters estimated are summarized in Table 2.

4 Monthly PDFs of soil moisture

Unfortunately the PDFs of the rainfall and the soil moisture models are not available analytically, as well as those for the combined rainfall–soil moisture model.

Thus, in this study, we generated the rainfall and the soil moisture time series using the combined rainfall–soil moisture model with the parameters estimated in the previous section.

Simulation of the soil moisture time series was based on Eq. 4, which is transformed into the following finite difference equation:

$$s(t+1) = \frac{C_1}{C_0} s(t) + \frac{C_2}{C_0} P(t+1) \tag{21}$$

where,

$$C_0 = 1 + \frac{\eta \Delta t}{2nZ_r} \tag{22}$$

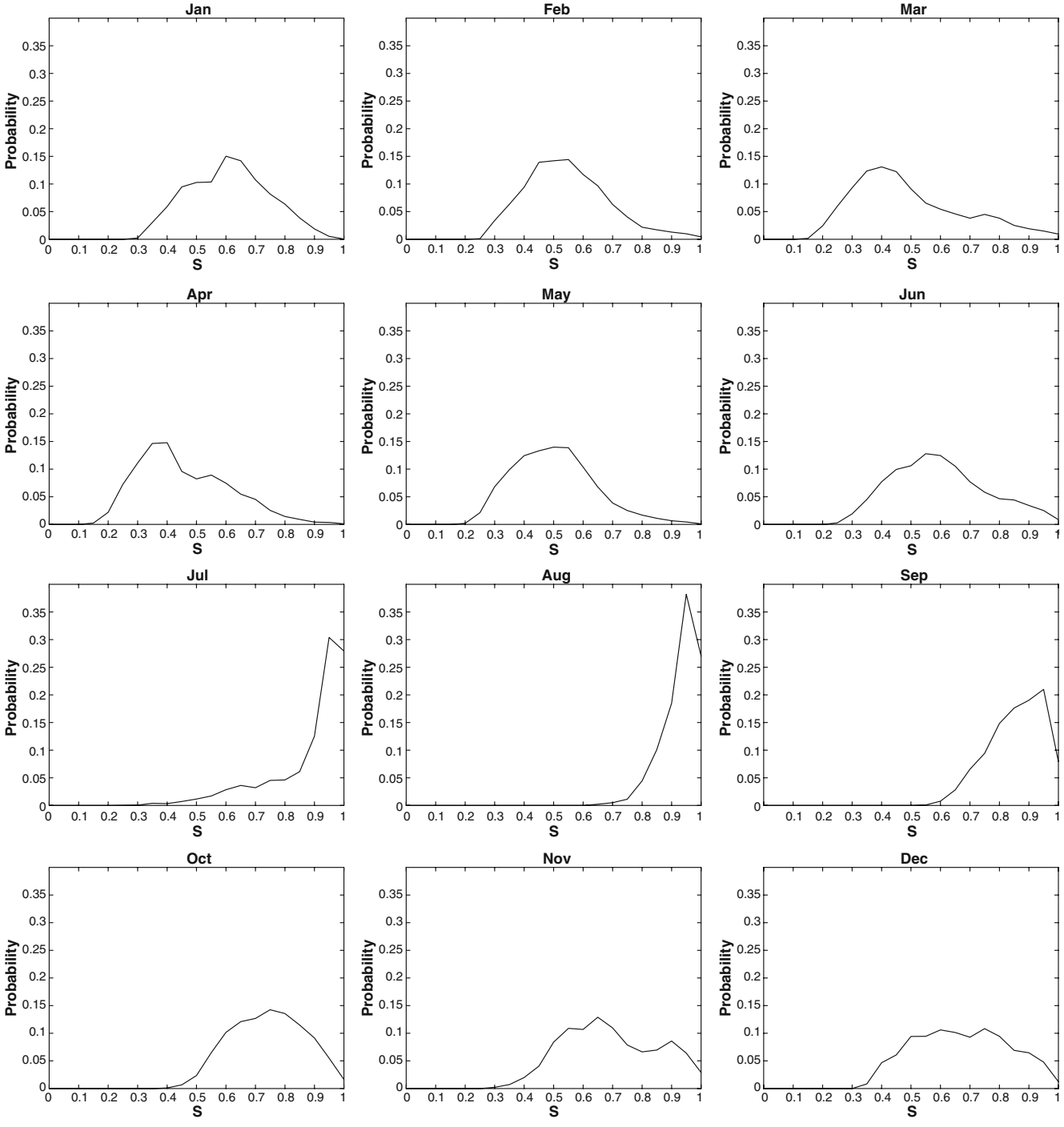

Fig. 4 Monthly probability density functions (PDFs) of soil moisture derived for the Seoul site

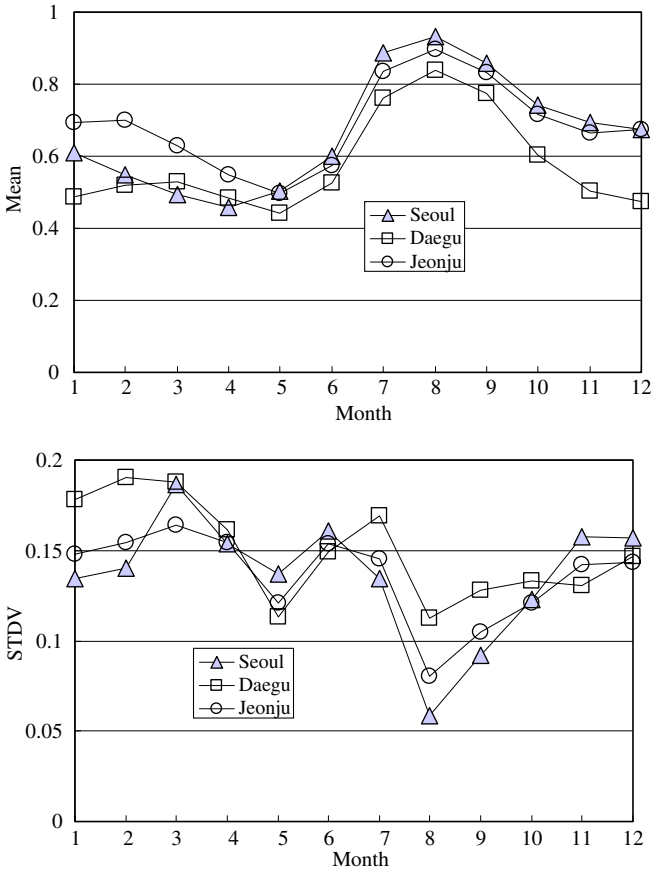

Fig. 5 Mean, standard deviation (*STDV*), and skewness of monthly soil moisture

$$C_1 = 1 - \frac{\eta \Delta t}{2nZ_r} \tag{23}$$

$$C_2 = \frac{\Delta t}{nZ_r.} \tag{24}$$

In this study, total 100 years of hourly time series of rainfall were generated and reserved to be used as an input for the generation of soil moisture. The same 100 years of hourly time series of soil moisture were then generated based on Eq. 21. All the simulations were conducted continuously by switching the model parameters every month, and then the resulting soil moisture time series were also quantified on a monthly basis to derive the monthly PDFs of soil moisture. A total of three sets of 12 PDFs were derived for each site considered, which were then analyzed and compared with respect to seasonality and drought vulnerability.

Figure 3 shows a part of the rainfall and soil moisture data generated for the Seoul site. As can be seen from this figure, soil moisture has obvious seasonality. Also the behavior of the soil moisture was realistic both in its decay pattern and its sensitivity to the rainfall forcing.

Figure 4 shows the PDFs derived based on the soil moisture data generated for the Seoul site (basic statistics are also summarized in Fig. 5 along with those for other sites considered). First of all, a strong seasonality in monthly PDFs of soil moisture is noticeable. Means of soil moisture are less than 0.5 during the dry spring season (March, April, and May), but other months are more than 0.5. In particular, the small soil moisture contents less than 0.5 in April and May seem to represent more vulnerability of Korean Peninsula to severe drought occurrences. Almost every 2 years, this region experiences mild droughts, and every 5–10 years more severe ones (it is called the spring drought in Korea). July and August show a very wet condition of soil moisture, but this condition decays slowly from September to May next year until the new wet season begins. Rather high soil moisture contents are also remained through the winter.

Another difference between the wet and dry seasons can be found in the shape of their PDFs. First, the dry months have rather large standard deviations compared with the wet months. It is the largest in March and the least in August. In most months, higher soil moisture content seems to lead to smaller standard deviation, but June and July are exceptions. These 2 months are affected by the Monsoon, which begins from the end of June and ends in mid-July.

Similar characteristics of monthly skewness can also be found. Basically, they are all skewed to be far from the Gaussian distribution. However, most wet months provide negatively skewed PDFs, but positively ones for the dry months. From June to July, the skewness suddenly changes from positive to negative, but recovers very slowly to become positive after the end of wet season. Overall, the spring season is characterized by the low mean value, high standard deviation, and positive skewness of the soil moisture content. On the other hand, the wet season is characterized by the high mean value, low standard deviation, and negative skewness of the soil moisture content. Thus, in the spring season, much drier soil moisture conditions can appear due to the higher variability and positive skewness of the soil moisture PDF, which also indicates more vulnerability of the Korean Peninsula to severe drought occurrence.

Figures 6 and 7 are the same results as in Fig. 4 but for the other sites; one is for Daegue and the other for Jeonju. Located about 200 km south from Seoul, both represent eastern and western parts of the Korean Peninsula, respectively. From these figures, we can easily see that the overall trends are similar, but a slightly different soil moisture contents. That is, Daegue shows obviously less soil moisture content than Jeonju for the whole year. Especially, far less soil moisture content during winter and spring is noticeable. This much lengthens the duration of less than 0.5 soil moisture contents in Daegue to 7 months. It is just 4 months and 1 month for Seoul and Jeonju, respectively. So, it is not difficult to conclude that the south-eastern part of the Korean Peninsular is most vulnerable to drought; the south-western part is least vulnerable to drought. These results are all coincident with the climatology of the Korean Peninsula.

5 Summary and comments

This study tried to statistically quantify and evaluate the condition of soil moisture as well as its seasonality. A zero-dimensional soil moisture dynamics model (Entekhabi and Rodriguez-Iturbe 1994) with the rainfall forcing by the rectangular pulses Poisson process model (Rodriguez-Iturbe et al. 1984) wais used for this study. First- and second-order moments of soil moisture were also reviewed for both instantaneous and locally averaged cases to link them to those of the rainfall, a link by which the impact of rainfall on the soil moisture could be evaluated. Finally, simulation study was carried out to estimate the PDF of soil moisture as well as to evaluate its seasonality.

Three sites (Seoul, Daegu, and Jeonju), representing the central, south-eastern, and south-western parts of the Korean Peninsula, were considered in this study. Mean, variance, and lag-1 auto-correlation coefficient

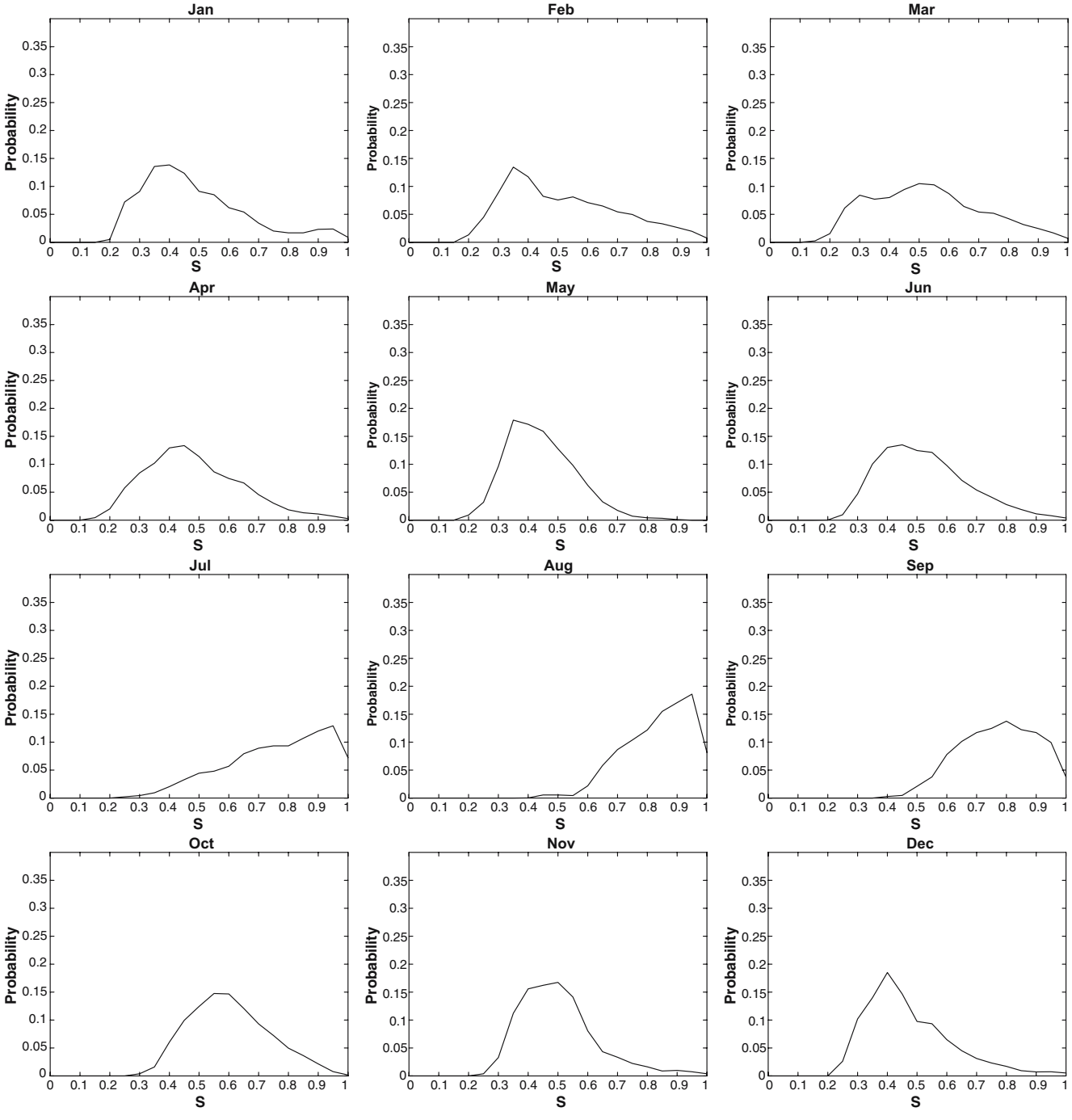

Fig. 6 Same as Fig. 4, but for the Daegue site

for 1-h rainfall data were used for the estimation of rainfall model parameters. On the other hand, the soil moisture model parameter was assumed to be the potential evaporation rate estimated by the Penmann method. All the parameters were estimated on a monthly basis, also the resulting soil moisture simulations were summarized on a monthly basis.

Results can be summarized as follows:

1. Strong seasonality of soil moisture could be observed in the simulations. The means of soil moisture are less than 0.5 during the dry spring season (March, April, and June), but more than 0.5 during the other months.
2. The spring season is characterized by the low mean value, high standard deviation, and positive skewness of soil moisture content. On the other hand, the wet season is characterized by the high mean value, low standard deviation, and negative skewness of soil moisture content. Thus, in the spring season, much drier soil moisture conditions can appear due to the higher variability and positive skewness of the soil

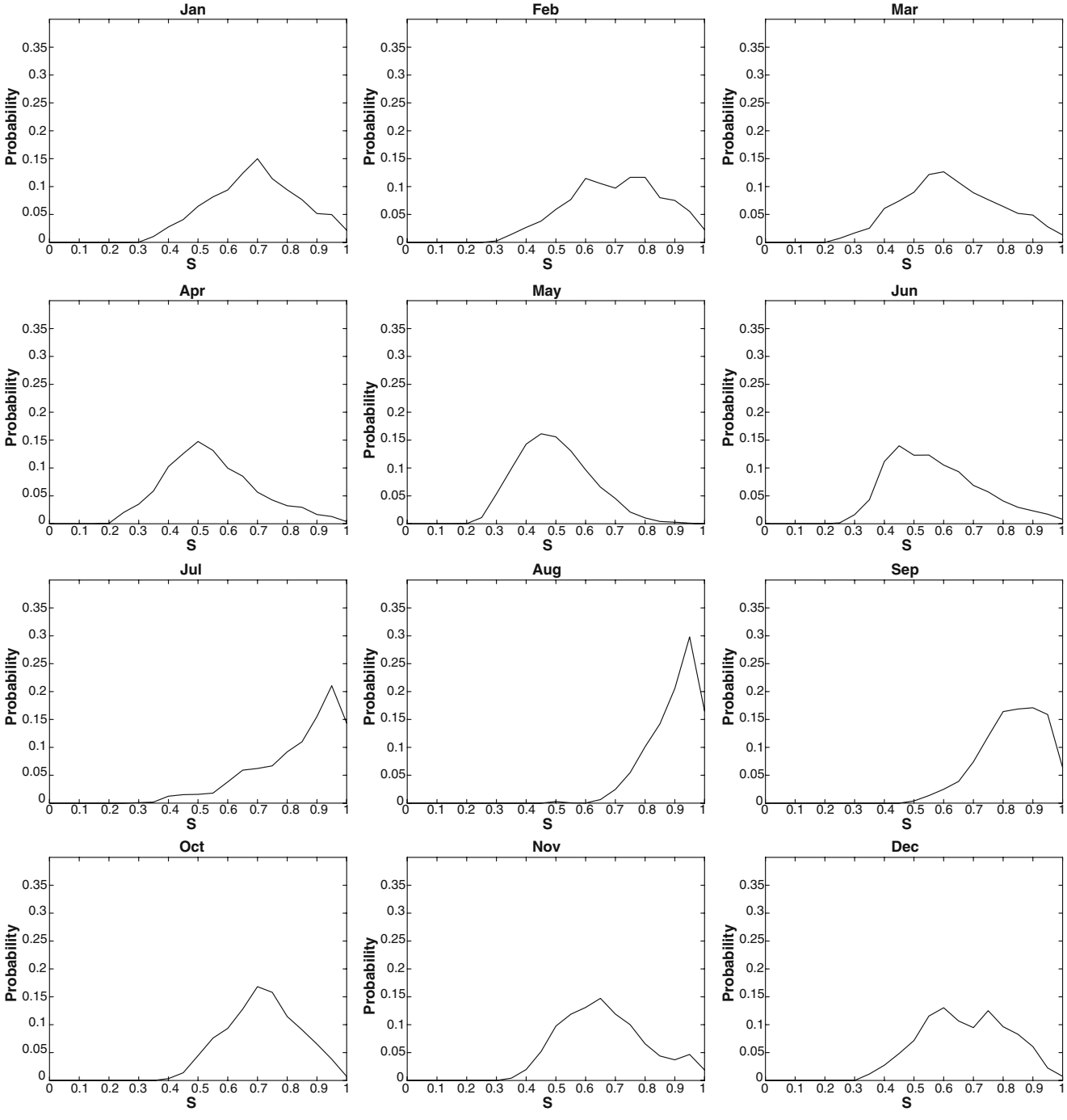

Fig. 7 Same as Fig. 4, but for the Jeonju site

moisture PDF, which also indicate more vulnerability of the Korean Peninsula to severe drought occurrence. This results is also coincident with the climate in Korea, which experiences mild droughts almost every 2 years, and more severe ones every 5–10 years.

3. Seoul, Daegue, and Jeonju show very similar overall trends of soil moisture variation. However, Daegue shows the least soil moisture content all through the year. This result shows that the south-eastern part of the Korean Peninsula is the most vulnerable to drought. On the other hand, the central part and the south-western part of the Korean Peninsula are less vulnerable to the risk of drought. These results are coincident with the climatology of the Korean Peninsula.

References

Bell KR, Blanchard BJ, Schmugge TJ, Witczak MW (1980) Analysis of surface moisture variations within large field sites. Water Resour Res 16(4):796–810

Byun HR (1996) On the atmospheric circulation caused drought in Korea. J Korea Meteorol Soc 32(3):455–469

Castelli F, Rodriguez-Iturbe I (1996) On the dynamical coupling of large scale spatial patterns of rainfall and soil moisture. Tellus 48(A):290–311

Cordova JR, Rodriguez-Iturbe I (1985) On the probabilistic structure of storm surface runoff. Water Resour Res 21(5):755–763

Entekhabi D, Rodriguez-Iturbe I (1994) Analytical framework for the characterization of the space-time variability of soil moisture. Adv Water Resour 17:35–45

Entekhabi D, Rodriguez-Iturbe I, Castelli F (1996) Mutual iinteraction of soil moisture state and atmospheric processes. J Hydrol 184:3–17

Han YH, Byun HR (1994) On the existence of seasonal drought in the Korean Peninsula. J Korea Meteorol Soc 30(3):457–467

Jackson TJ, Le Vine DE (1996) Mapping surface soil moisture using an aircraft-based passive microwave instrument: algorithm and example. J Hydrol 184:85–99

Korea Water Resources Coporation (KOWACO) (2002) Study on comprehensive drought management. Daejeon, pp 554

Kustas WP, Goodrich DD (1994) Preface. Water Resour Res 30(5):1211–1225

Njoku E, Entekhabi D (1996) Passive microwave remote sensing of soil moisture. J Hydrol 184:101–129

North GR, Nakamoto S (1989) Formalism for comparing rain estimation designs. J Atmos Ocean Tech 6:985–992

Rhee DY (1998) Relationship between El Nino/Southern oscillation and Korean drought. J Korean Assoc Civil Eng 18(2):67–70

Rodriguez-Iturbe I (1986) Scale of fluctuation of rainfall models. Water Resour Res 22(9):15S–37S

Rodriguez-Iturbe I, Gupta VK, Waymire E (1984) Scale considerations in the modeling of temporal rainfall. Water Resour Res 20(11):1611–1619

Yoo C (2001) Sampling of soil moisture fields and related errors: implications to the optimal sampling design. Adv Water Resour 24(5):521–530

Yoo C, Valdes JB, North GR (1998) Evaluation of the impact of rainfall on soil moisture variability. Adv Water Resour 21(5):375–384

Yoo C, Kim Seong J, Lee J-S (2001) Land cover change and its impact on soil-moisture-field evolution. J Hydrol Eng ASCE 6(5):436–441

Yoo C, Kim S-J, Valdes JB(2005) Sensitivity of soil moisture field evolution on rainfall forcing. Hydrol Processes 19:1855–1869